Journal of Magnetic Resonance 318 (2020) 106783

Contents lists available at ScienceDirect

Journal of Magnetic Resonance

journal homepage: www.elsevier.com/locate/jmr

^{1}H spin-lattice NMR relaxation in the presence of residual dipolar interactions – Dipolar relaxation enhancement

Danuta Kruk [a,*], Pawel Rochowski [a,1], Malgorzata Florek – Wojciechowska [b], Pedro José Sebastião [c], David J. Lurie [d], Lionel M. Broche [d]

[a] Faculty of Mathematics and Computer Science, University of Warmia & Mazury in Olsztyn, Słoneczna 54, 10-710 Olsztyn, Poland
[b] Department of Physics & Biophysics, University of Warmia and Mazury in Olsztyn, Oczapowskiego 4, 11-041 Olsztyn, Poland
[c] Department of Physics, Instituto Superior Técnico, Universidade de Lisboa, Av. Rovisco Pais, 1049-001 Lisbon, Portugal
[d] Bio-Medical Physics, School of Medicine, Medical Sciences & Nutrition, University of Aberdeen, Foresterhill, Aberdeen AB25 2ZD, Scotland, United Kingdom

ARTICLE INFO

Article history:
Received 4 April 2020
Revised 29 June 2020
Accepted 5 July 2020
Available online 13 July 2020

Keywords:
NMR
Relaxation
Dynamics

ABSTRACT

A model of spin-lattice relaxation for spin-1/2 nuclei in the presence of a residual dipole-dipole coupling has been presented. For slow dynamics the model predicts a bi-exponential relaxation at low frequencies, when the residual dipole-dipole interaction dominates the Zeeman coupling. Moreover, according to the model a frequency-specific relaxation enhancement, referred to as Dipolar Relaxation Enhancement (DRE) in analogy to the Quadrupole Relaxation Enhancement (QRE) is expected. The frequency position of the relaxation maximum is determined by the amplitude of the residual dipole-dipole interaction. Experimental examples of relaxation properties that might be attributed to the DRE are presented. The DRE effect has the potential to be exploited, in analogy to QRE, as a unique source of information about molecular dynamics and structure.

1. Introduction

The potential of NMR relaxation studies to reveal dynamical properties of molecular and ionic systems is widely known. However, the information provided by relaxation experiments performed only at a single resonance frequency (magnetic field) is limited to dynamical processes occurring on the time scale of the reciprocal frequency. In this respect, Fast Field-Cycling (FFC) technology [1,2] introduced (literally speaking) a new dimension to NMR relaxation studies – namely, the possibility to vary the magnetic field in a very broad range: from about 1 kHz to 120 MHz (referring to ^{1}H resonance frequency). NMR relaxation experiments performed versus the resonance frequency are often referred to as NMR relaxometry, while relaxation rates (spin-lattice or spin-spin) plotted as a function of the frequency are called relaxation dispersion profiles.

The first great advantage of NMR relaxometry is the opportunity to probe in a single experiment dynamical processes on a time scale from ms to ns, independently of the mechanism of the motion [3-5]. The second, unique advantage of this method is the possibility to unambiguously determine the mechanism of motion [3-9]. According to spin relaxation theories [10-15], relaxation rates are given as linear combinations of spectral density functions being Fourier transforms of the corresponding time correlation function characterizing the dynamical process causing stochastic fluctuations of the spin interactions that lead to relaxation. As the mathematical form of the correlation function (and, hence, the spectral density) depends on the mechanism of motion (like isotropic and anisotropic rotation and translation), the shape of the relaxation dispersion profile reflects the nature of the dynamics [16-26].

Progress in NMR relaxometry has led to an extensive development of spin relaxation theories. The "classical" relaxation theory [10-14] assumes that the energy level structure of the spin system is entirely determined by the Zeeman interaction. This assumption holds only at high magnetic fields, because then other spin couplings, like quadrupole interaction, zero field splitting for paramagnetic systems or dipole-dipole interactions, are negligible compared to the Zeeman interaction. Relaxation models based on this assumption break down, for obvious reasons, at low and intermediate magnetic fields when other spin interactions become comparable with the Zeeman coupling.

The remarkable experimental opportunities offered by FFC technology pose a great theoretical challenge from the viewpoint of providing appropriate theoretical models including complex

* Corresponding author.
E-mail address: danuta.kruk@matman.uwm.edu.pl (D. Kruk).
[1] Current affiliation: Faculty of Mathematics, Physics and Informatics, University of Gdansk, Wita Stwosza 57, PL-80308 Gdansk, Poland.

https://doi.org/10.1016/j.jmr.2020.106783
1090-7807/

quantum-mechanical effects caused by an interplay between different spin interactions. One of the effects is the so called Quadrupole Relaxation Enhancement (QRE) [21,27-39]. The QRE manifests itself as frequency specific maxima of the ^{1}H or ^{19}F spin-lattice relaxation rates referred to as quadrupole peaks. The maxima are associated with dipole-dipole interactions between spin-1/2 nuclei ($I = 1/2$) and nuclei of the spin quantum number $S \geq 1$ possessing a quadrupole moment. For slow dynamics the energy level structure of the S-spin nucleus (for instance ^{14}N) is determined by a superposition of its quadrupole and Zeeman interactions. This implies that at some magnetic fields the resonance frequency of the spin-1/2 nucleus matches the transition frequencies of the S-spin nucleus between its energy levels. At these magnetic fields the I-spin magnetization can be taken over by (transferred to) the S-spin. The faster decay of the I-spin magnetization can be interpreted as a frequency specific increase of the relaxation rate. This scenario should be considered as a limiting case, because QRE effects are also observed for intermediate-scale dynamics, however, then the theoretical model is much more cumbersome [21,27-31], because one cannot treat the quadrupole coupling as a time independent contribution to the energy level structure. The effort put into the development of the theory of QRE effects has turned out to be highly rewarding. The quadrupole peaks have been observed for a variety of systems, from ionic and molecular solids of different kinds [27-29] via proteins [32-34] to tissues [34-36]. In the last case, the QRE effects are considered as potentially important diagnostic biomarkers for use with FFC magnetic resonance imaging (MRI) [35,37]. The QRE effects have also given rise to a completely new concept of MRI contrast [38-40].

In this paper we consider the influence of residual dipole-dipole interactions between spin-1/2 nuclei on their spin-lattice relaxation at low fields. Residual (time-independent) dipole-dipole interactions are expected to be mainly present in solids and macromolecules, including biomolecules. The work can be treated as a continuation of the efforts to formulate theoretical models of spin relaxation processes beyond the high-field limit. One should be aware that the theoretically-predicted effects of residual dipole-dipole interactions are much more difficult to observe experimentally than QRE. The reason for that is twofold: first, not only specific conditions regarding the time scale of dynamical processes must be met, but also the dynamics must be anisotropic to create a residual dipole-dipole coupling; second, the effects are supposed to be present at low fields when the experimental procedures are much more demanding and the relaxation rates often reach the limit of FFC relaxometers. Nevertheless, we are of the opinion that it is important to become aware of the effect (in analogy to QRE we shall call it Dipolar Relaxation Enhancement, DRE) because if detected and properly theoretically modeled it has a potential as a source of information about molecular dynamics and can turn out to be an important factor for materials science studies and medical diagnosis based on the FFC technique.

2. Theory

Let us consider two protons of spin quantum numbers $I_1 = I_2 = 1/2$ placed in a low, external magnetic field, $\vec{B}_0$, and coupled by a dipole-dipole interaction represented by a Hamiltonian $H_{DD}(I_1, I_2)$. The dipole-dipole Hamiltonian can be split into two parts:

$$H_{DD}(t) = \langle H_{DD}(t)\rangle + \left(H_{DD}(t) - \langle H_{DD}(t)\rangle\right) = H_{DD}^{res} + H_{DD}^{fluc}(t) \quad (1)$$

The first term, $\langle H_{DD}(t)\rangle = H_{DD}^{res}$, describes a part of the dipole-dipole interactions being a result of a long time averaging. This term is referred to as a residual dipolar coupling and its non-zero value is caused by anisotropy of molecular motion. The residual dipolar interaction does not fluctuate in time with respect to the laboratory frame. The second term, $H_{DD}^{(L),fluc}(t)$, describes the stochastically fluctuating part of the dipole-dipole interaction. The concept of splitting the total dipole-dipole coupling into the residual and fluctuating parts can be described in terms of a time correlation function $C(t)$. According to the Lipari-Szabo model [12,41], for molecules experiencing a local, anisotropic dynamics and undergoing at the same time an overall motion on a much longer time scale, the correlation function takes the form (assuming exponential correlation functions for both dynamical contributions): $C(t) = \left(1 - S^2\right)\exp(-t/\tau_f) + S^2\exp(-t/\tau_s)$, where τ_f and τ_s denote correlation times of the fast and slow dynamical processes, respectively; S^2 is referred to as an order parameter. This formula means that in the first step (in a short time) the correlation function decays from unity to the S value as a result of the fast, anisotropic motion, and then, in the second step, it eventually decays to zero at long times due to the slow motion. When $\tau_s >> T_1$ (T_1 denotes the spin-lattice relaxation time) the slow process is not seen and one can write: $C(t) = \left(1 - S^2\right)\exp(-t/\tau_c) + S^2$, where the first term corresponds to the Hamiltonian $H_{DD}^{fluc}(t)$ fluctuating with a correlation time $\tau_c = \tau_f$, while S reflects the presence of the time independent residual dipole-dipole coupling, H_{DD}^{res}. The explicit form of the H_{DD}^{res} Hamiltonian expressed in the laboratory (L) frame determined by the direction of the external magnetic field, yields [15,42,43]:

$$H_{DD}^{res}(I_1, I_2) = C^{res}\sum_{m=-2}^{2}(-1)^m D_{0,-m}^{2}(\theta_{ML}, \phi_{ML})T_m^2(I_1, I_2) \quad (2)$$

where C^{res} is the amplitude of the residual dipolar coupling, while the angles $\theta_{ML} = \theta$ and $\phi_{ML} = \phi$ describe the orientation of a molecule fixed frame (M) with respect to the laboratory frame (L). For simplicity the principal axes system of the residual dipolar coupling is chosen as the molecular frame. The spin tensor operators are defined as: $T_0^2(I_1, I_2) = \frac{1}{\sqrt{6}}\left[2I_{1z}I_{2z} - \frac{1}{2}(I_{1+}I_{2-} + I_{1-}I_{2+})\right]$, $T_{\pm1}^2(I_1, I_2) = \mp\frac{1}{2}(I_{1z}I_{2\pm} + I_{1\pm}I_{2z})$, $T_{\pm2}^2(I_1, I_2) = \frac{1}{2}I_{1\pm}I_{2\pm}$, while the Wigner rotation matrices are given as [15,42,43]: $D_{0,0}^2(\theta, \phi) = \frac{1}{2}\left(3\cos^2\theta - 1\right)$, $D_{0,\pm1}^2(\theta, \phi) = \mp\sqrt{\frac{3}{2}}\cos\theta\sin\theta\exp(\pm i\phi)$, $D_{0,\pm2}^2(\theta, \phi) = \mp\sqrt{\frac{3}{8}}\sin^2\theta\exp(\pm 2i\phi)$. The main Hamiltonian, determining the energy level structure of the pair of spins, $I_1 - I_2$, consists of the Zeeman Hamiltonians of these spins and H_{DD}^{res}; assuming that the spins are equivalent, it yields: $H_0(I_1, I_2) = \omega(I_{1z} + I_{2z}) + H_{DD}^{res}(I_1, I_2)$, where ω denotes the resonance frequency of the spins. The energy levels can be obtained by diagonalizing the matrix representation of the Hamiltonian in the basis $\{|n\rangle = |m_1, m_2\rangle\}$, where m_1 and m_2 are magnetic quantum numbers of the spins I_1 and I_2, respectively. We shall refer to this basis as a Zeeman basis as it is formed from the eigenfunctions of the Zeeman Hamiltonian. Introducing the labelling: $|1\rangle = \left|\frac{1}{2}, \frac{1}{2}\right\rangle$, $|2\rangle = \left|\frac{1}{2}, -\frac{1}{2}\right\rangle$, $|3\rangle = \left|-\frac{1}{2}, \frac{1}{2}\right\rangle$, $|4\rangle = \left|-\frac{1}{2}, -\frac{1}{2}\right\rangle$, one obtains:

$$[H_0(I_1, I_2)(\theta, \phi)] = \begin{bmatrix} \omega + \frac{C^{res}}{2\sqrt{6}}D_{0,0}^2 & -\frac{C^{res}}{4}D_{0,-1}^2 & -\frac{C^{res}}{4}D_{0,-1}^2 & \frac{C^{res}}{2}D_{0,-2}^2 \\ \frac{C^{res}}{4}D_{0,1}^2 & -\frac{C^{res}}{2\sqrt{6}}D_{0,0}^2 & -\frac{C^{res}}{2\sqrt{6}}D_{0,0}^2 & \frac{C^{res}}{4}D_{0,-1}^2 \\ \frac{C^{res}}{4}D_{0,1}^2 & -\frac{C^{res}}{2\sqrt{6}}D_{0,0}^2 & -\frac{C^{res}}{2\sqrt{6}}D_{0,0}^2 & \frac{C^{res}}{4}D_{0,-1}^2 \\ \frac{C^{res}}{2}D_{0,2}^2 & -\frac{C^{res}}{4}D_{0,1}^2 & -\frac{C^{res}}{4}D_{0,1}^2 & -\omega + \frac{C^{res}}{2\sqrt{6}}D_{0,0}^2 \end{bmatrix} \quad (4)$$

The energy levels of the $I_1 - I_2$ spin system are then given by the eigenvalues, $E_\alpha(\theta, \phi)$, of the Hamiltonian matrix of Eq.4, while the corresponding eigenfunctions $|\psi_\alpha\rangle = \sum_{n=1}^{4} c_{\alpha n}(\theta, \phi)|n\rangle$ are expressed

as linear combinations of the $|n\rangle = |m_1, m_2\rangle$ functions. The functions $\{|\alpha\rangle\}$ form the eigenbasis of the spin system, while their pairs $\left\{|\psi_\alpha\rangle\langle\psi_\beta| = \tilde{\rho}_{\alpha\beta}\right\}$ give a set of coherences evolving in time according to the Redfield relaxation theory, *i.e.* following the set of equations [11,12,14,15,43-46]:

$$\begin{aligned}\tilde{R}_{\alpha\alpha\beta\beta} = \left(C^{fluc}\right)^2 * \{&\tfrac{1}{12}\left(c^*_{\alpha1}c_{\beta1} - c^*_{\alpha2}c_{\beta2} - c^*_{\alpha3}c_{\beta3} + c^*_{\alpha4}c_{\beta4} - c^*_{\alpha2}c_{\beta3} - c^*_{\alpha3}c_{\beta2}\right)^2\\ &+\tfrac{1}{8}\left(-c^*_{\alpha1}c_{\beta2} - c^*_{\alpha1}c_{\beta3} + c^*_{\alpha2}c_{\beta4} + c^*_{\alpha3}c_{\beta4}\right)^2\\ &+\tfrac{1}{8}\left(c^*_{\alpha2}c_{\beta1} + c^*_{\alpha3}c_{\beta1} - c^*_{\alpha4}c_{\beta2} - c^*_{\alpha4}c_{\beta3}\right)^2\\ &+\tfrac{1}{2}\left(c^*_{\alpha1}c_{\beta4}\right)^2 + \tfrac{1}{2}\left(c^*_{\alpha4}c_{\beta1}\right)^2\}J(\omega_{\alpha\beta})\end{aligned} \tag{9a}$$

$$\begin{aligned}\tilde{R}_{\alpha\beta\alpha\beta} = \left(C^{fluc}\right)^2 * [&-\{\tfrac{1}{24}\left(c^*_{\alpha1}c_{\alpha1} - c^*_{\alpha2}c_{\alpha2} - c^*_{\alpha3}c_{\alpha3} + c^*_{\alpha4}c_{\alpha4} - c^*_{\alpha2}c_{\alpha3} - c^*_{\alpha3}c_{\alpha2} - c^*_{\beta1}c_{\beta1} + c^*_{\beta2}c_{\beta2} + c^*_{\beta3}c_{\beta3} - c^*_{\beta4}c_{\beta4} + c^*_{\beta2}c_{\beta3} + c^*_{\beta3}c_{\beta2}\right)^2\\ &+\tfrac{1}{16}\left(-c^*_{\alpha1}c_{\alpha2} - c^*_{\alpha1}c_{\alpha3} + c^*_{\alpha2}c_{\alpha4} + c^*_{\alpha3}c_{\alpha4} + c^*_{\beta1}c_{\beta2} + c^*_{\beta1}c_{\beta3} - c^*_{\beta2}c_{\beta4} - c^*_{\beta3}c_{\beta4}\right)^2\\ &+\tfrac{1}{4}\left(c^*_{\alpha1}c_{\alpha4} - c^*_{\beta1}c_{\beta4}\right)^2\}J(0) - \sum_{\gamma=1,\gamma\neq\alpha}^{4}\{\tfrac{1}{24}\left(c^*_{\alpha1}c_{\gamma1} - c^*_{\alpha2}c_{\gamma2} - c^*_{\alpha3}c_{\gamma3} + c^*_{\alpha4}c_{\gamma4} - c^*_{\alpha2}c_{\gamma3} - c^*_{\alpha3}c_{\gamma2}\right)^2 + \tfrac{1}{16}\left(-c^*_{\alpha1}c_{\gamma2} - c^*_{\alpha1}c_{\gamma3} + c^*_{\alpha2}c_{\gamma4} + c^*_{\alpha3}c_{\gamma4}\right)^2\\ &+\tfrac{1}{16}\left(c^*_{\alpha2}c_{\gamma1} + c^*_{\alpha3}c_{\gamma1} - c^*_{\alpha4}c_{\gamma2} - c^*_{\alpha4}c_{\gamma3}\right)^2 + \tfrac{1}{4}\left(c^*_{\alpha1}c_{\gamma4}\right)^2 + \tfrac{1}{4}\left(c^*_{\alpha4}c_{\gamma1}\right)^2\}J(\omega_{\gamma\alpha})\\ &- \sum_{\gamma=1,\gamma\neq\beta}^{4}\{\tfrac{1}{24}\left(c^*_{\beta1}c_{\gamma1} - c^*_{\beta2}c_{\gamma2} - c^*_{\beta3}c_{\gamma3} + c^*_{\beta4}c_{\gamma4} - c^*_{\beta2}c_{\gamma3} - c^*_{\beta3}c_{\gamma2}\right)^2\\ &+\tfrac{1}{16}\left(-c^*_{\beta1}c_{\gamma2} - c^*_{\beta1}c_{\gamma3} + c^*_{\beta2}c_{\gamma4} + c^*_{\beta3}c_{\gamma4}\right)^2 + \tfrac{1}{16}\left(c^*_{\beta2}c_{\gamma1} + c^*_{\beta3}c_{\gamma1} - c^*_{\beta4}c_{\gamma2} - c^*_{\beta4}c_{\gamma3}\right)^2\\ &+\tfrac{1}{4}\left(c^*_{\beta1}c_{\gamma4}\right)^2 + \tfrac{1}{4}\left(c^*_{\beta4}c_{\gamma1}\right)^2\}J(\omega_{\gamma\beta})\,]\end{aligned} \tag{9b}$$

$$\frac{d\tilde{\rho}_{\alpha\alpha'}(t)}{dt} = -i\omega_{\alpha\alpha'}\tilde{\rho}_{\alpha\alpha'}(t) + \sum_{\beta\beta'\ \ \omega_{\alpha\alpha'}=\omega_{\beta\beta'}} \tilde{R}_{\alpha\alpha'\beta\beta'}\tilde{\rho}_{\beta\beta'}(t) \tag{5}$$

where $\omega_{\alpha\alpha'} = E_\alpha - E_{\alpha'}$. According to the Redfield relaxation theory the $\tilde{R}_{\alpha\alpha'\beta\beta'}$ coefficients are given by the well-known expression [11,12,14,15,43-46]:

$$\tilde{R}_{\alpha\alpha'\beta\beta'} = \tilde{\Im}_{\alpha\beta\alpha'\beta'}(\omega_{\alpha\beta}) + \tilde{\Im}_{\alpha\beta\alpha'\beta'}(\omega_{\beta'\alpha'}) - \delta_{\alpha'\beta'}\sum_\gamma \tilde{\Im}_{\alpha\gamma\beta\gamma}(\omega_{\gamma\beta}) - \delta_{\alpha\beta} \times \sum_\gamma \tilde{\Im}_{\beta'\gamma\alpha'\gamma}(\omega_{\beta'\gamma}) \tag{6}$$

where the quantities $\tilde{\Im}_{\alpha\beta\alpha'\beta'}(\omega)$ are defined as:

$$\tilde{\Im}_{\alpha\beta\alpha'\beta'}(\omega) = \langle\psi_\alpha|H^{fluc}_{DD}|\psi_\beta\rangle\langle\psi_{\alpha'}|H^{fluc}_{DD}|\psi_{\beta'}\rangle J(\omega) \tag{7}$$

where $J(\omega) = \frac{1}{5}\frac{\tau_c}{1+\omega^2\tau_c^2}$ assuming an exponential correlation function [10,12,15]. To calculate the relaxation rates $\tilde{R}_{\alpha\alpha'\beta\beta'}$ for the individual coherences the matrix representation of the perturbing Hamiltonian, $H^{fluc}_{DD}(I_1, I_2)(t) = C^{fluc}\sum_{m=-2}^{2}(-1)^m D^2_{0,-m}(t)T^2_m(I_1, I_2)$ is needed. The representation of $H^{fluc}_{DD}(t)$ in the Zeeman basis, $\{|n\rangle = |m_1, m_2\rangle\}$, has the form:

$$\left[H^{fluc}_{DD}(I_1, I_2)(t)\right] = C^{fluc} * \begin{bmatrix} \frac{D^2_{0,0}(t)}{2\sqrt{6}} & -\frac{D^2_{0,-1}(t)}{4} & -\frac{D^2_{0,-1}(t)}{4} & \frac{D^2_{0,-2}(t)}{2} \\ \frac{D^2_{0,1}(t)}{4} & -\frac{D^2_{0,0}(t)}{2\sqrt{6}} & -\frac{D^2_{0,0}(t)}{2\sqrt{6}} & \frac{D^2_{0,-1}(t)}{4} \\ \frac{D^2_{0,1}(t)}{4} & -\frac{D^2_{0,0}(t)}{2\sqrt{6}} & -\frac{D^2_{0,0}(t)}{2\sqrt{6}} & \frac{D^2_{0,-1}(t)}{4} \\ \frac{D^2_{0,2}(t)}{2} & -\frac{D^2_{0,1}(t)}{4} & -\frac{D^2_{0,1}(t)}{4} & \frac{D^2_{0,0}(t)}{2\sqrt{6}} \end{bmatrix} \tag{8}$$

Using the relationship, $|\psi_\alpha\rangle = \sum_{n=1}^{4} c_{\alpha n}(\theta,\phi)|n\rangle$, one can write: $\langle\psi_\alpha|H^{fluc}_{DD}(t)|\psi_\beta\rangle = \sum_{n,k=1}^{4} c^*_{\alpha n}(\theta,\phi)c_{\beta k}(\theta,\phi)\langle n|H^{fluc}_{DD}(t)|k\rangle$. This implies that the relaxation matrix elements can be expressed as:

and $\tilde{R}_{\alpha\alpha\alpha\alpha} = -\sum_{\beta\neq\alpha}\tilde{R}_{\alpha\alpha\beta\beta}$. The elements form the 16×16 relaxation matrix in the Liouville space constructed from the pairs of the eigenfunctions $\left\{|\psi_\alpha\rangle\langle\psi_\beta| = \tilde{\rho}_{\alpha\beta}\right\}$. The $\tilde{\rho}_{\alpha\alpha}$ coherences are associated with the population block, while the other twelve coherences, $\tilde{\rho}_{\alpha\beta}$, $\alpha\neq\beta$, correspond to the diagonal part of the relaxation matrix. Eq. (5) can be rewritten in the form:

$$\frac{d}{dt}\left[\tilde{\rho}\right] = -\left[\tilde{\Gamma}\right]\left[\tilde{\rho}\right] \tag{10}$$

where $\tilde{\Gamma}_{\alpha\beta\alpha'\beta'} = -i\omega_{\alpha\alpha'} + \tilde{R}_{\alpha\beta\alpha'\beta'}$. The relation between the coherences in the eigenbasis and the Zeeman basis is given as: $\tilde{\rho}_{\alpha\beta} = \sum_{n,k=1}^{4} c^*_{\alpha n}c_{\beta k}\rho_{nk}$. This relation can be written in a matrix form: $\left[\tilde{\rho}\right] = [A][\rho]$, where the transformation matrix, [A], includes the elements $c^*_{\alpha n}c_{\beta k}$. This implies, that Eq.10 takes in the Zeeman basis the form:

$$\frac{d}{dt}[\rho] = -\left([A]^{-1}\left[\tilde{\Gamma}\right][A]\right)[\rho] \tag{11}$$

From this equation the time evolution of the longitudinal component of the magnetization can be determined, for a given orientation of the residual dipolar coupling with respect to the laboratory frame, taking into account that $\langle I_z\rangle = \langle I_{z,1} + I_{z,2}\rangle \propto \rho_{44} - \rho_{11}$.

3. Simulations for the special case of $\theta = 0$, ϕ=0

When the principal axes system of the residual dipolar coupling coincides with the laboratory frame) the energy levels and the corresponding eigenfunctions can be expressed in the simple analytical form:

$$E_1 = \omega + \omega_{DD}, \qquad |\psi_1\rangle = |1\rangle = \left|\frac{1}{2}, \frac{1}{2}\right\rangle \tag{12a}$$

$$E_2 = 0, \qquad |\psi_2\rangle = \frac{1}{\sqrt{2}}(|2\rangle - |3\rangle)$$
$$= \frac{1}{\sqrt{2}}\left(\left|\frac{1}{2},-\frac{1}{2}\right\rangle - \left|-\frac{1}{2},\frac{1}{2}\right\rangle\right) \tag{12b}$$

$$E_3 = -2\omega_{DD}, \qquad |\psi_3\rangle = \frac{1}{\sqrt{2}}(|2\rangle + |3\rangle)$$
$$= \frac{1}{\sqrt{2}}\left(\left|\frac{1}{2},-\frac{1}{2}\right\rangle + \left|-\frac{1}{2},\frac{1}{2}\right\rangle\right) \tag{12c}$$

$$E_4 = -\omega + \omega_{DD}, \qquad |\psi_4\rangle = |4\rangle = \left|-\frac{1}{2},-\frac{1}{2}\right\rangle \tag{12d}$$

where $\omega_{DD} = \frac{C^{res}}{2\sqrt{6}}$. In consequence one obtains the following set of equations for the evolution of the population block of the spin coherences, $\rho_{\alpha\alpha}$, in the laboratory frame:

$$\begin{aligned}\frac{d\rho_{11}}{dt} = &-\left[\tfrac{1}{4}J(\omega+3\omega_{DD})+\tfrac{1}{2}J(2\omega)\right]\rho_{11}\\ &+\tfrac{1}{8}J(\omega+3\omega_{DD})\rho_{22}+\tfrac{1}{8}J(\omega+3\omega_{DD})\rho_{33}\\ &+\tfrac{1}{2}J(2\omega)\rho_{44}+\tfrac{1}{8}J(\omega+3\omega_{DD})\rho_{23}+\tfrac{1}{8}J(\omega+3\omega_{DD})\rho_{32}\end{aligned} \tag{13a}$$

$$\begin{aligned}\frac{d\rho_{22}}{dt} = &-i\omega_{DD}\rho_{23}+i\omega_{DD}\rho_{32}+\tfrac{1}{8}J(\omega+3\omega_{DD})\rho_{11}\\ &-\left[\tfrac{1}{8}J(\omega+3\omega_{DD})+\tfrac{1}{8}J(\omega-3\omega_{DD})+\tfrac{1}{12}J(0)\right]\rho_{22}\\ &+\tfrac{1}{12}J(0)\rho_{33}+\tfrac{1}{8}J(\omega-3\omega_{DD})\rho_{44}\\ &-\left[\tfrac{1}{16}J(\omega+3\omega_{DD})+\tfrac{1}{16}J(\omega-3\omega_{DD})\right]\rho_{23}\\ &-\left[\tfrac{1}{16}J(\omega+3\omega_{DD})+\tfrac{1}{16}J(\omega-3\omega_{DD})\right]\rho_{32}\end{aligned} \tag{13b}$$

$$\begin{aligned}\frac{d\rho_{33}}{dt} = &\,i\omega_{DD}\rho_{23}-i\omega_{DD}\rho_{32}+\tfrac{1}{8}J(\omega+3\omega_{DD})\rho_{11}+\tfrac{1}{12}J(0)\rho_{22}\\ &-\left[\tfrac{1}{8}J(\omega+3\omega_{DD})+\tfrac{1}{8}J(\omega-3\omega_{DD})+\tfrac{1}{12}J(0)\right]\rho_{33}\\ &+\tfrac{1}{8}J(\omega-3\omega_{DD})\rho_{44}\\ &-\left[\tfrac{1}{16}J(\omega+3\omega_{DD})+\tfrac{1}{16}J(\omega-3\omega_{DD})\right]\rho_{23}\\ &-\left[\tfrac{1}{16}J(\omega+3\omega_{DD})+\tfrac{1}{16}J(\omega-3\omega_{DD})\right]\rho_{32}\end{aligned} \tag{13c}$$

$$\begin{aligned}\frac{d\rho_{44}}{dt} = &\,\tfrac{1}{2}J(2\omega)\rho_{11}+\tfrac{1}{8}J(\omega-3\omega_{DD})\rho_{22}+\tfrac{1}{8}J(\omega-3\omega_{DD})\rho_{33}\\ &-\left[\tfrac{1}{4}J(\omega-3\omega_{DD})+\tfrac{1}{2}J(2\omega)\right]\rho_{44}\\ &+\tfrac{1}{8}J(\omega-3\omega_{DD})\rho_{23}+\tfrac{1}{8}J(\omega-3\omega_{DD})\rho_{32}\end{aligned} \tag{13d}$$

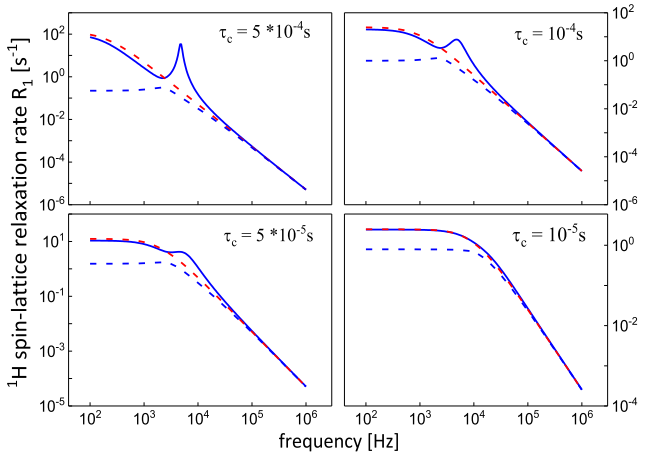

Fig. 1. ^{1}H spin-lattice relaxation rates for a model system consisting of two spins ½. Blue lines (solid and dashed) show two components of bi-exponential relaxation process in the presence of a residual dipolar coupling of $\omega_{DD} = 1 * 10^4$ rad/s for different correlation times, τ_c, and $C_{DD} = 1 * 10^3$ Hz. Red lines – predictions of the "classical" relaxation theory (in the absence of residual dipolar interactions). For fast dynamics and/or a weak residual dipolar coupling both blue lines converge to a single-exponential relaxation process represented by red lines. (For interpretation of the references to colour in this figure legend, the reader is referred to the web version of this article.)

The population block of the coherences, $\rho_{\alpha\alpha}$, is coupled also to the ρ_{23} and ρ_{32} (as expected due to the degeneracy of the states $|2\rangle$ and $|3\rangle$ in the Zeeman basis), but, at the same time decoupled from other coherences:

$$\begin{aligned}\frac{d\rho_{23}}{dt} = &-i\omega_{DD}\rho_{22}+i\omega_{DD}\rho_{33}+\tfrac{1}{8}J(\omega+3\omega_{DD})\rho_{11}\\ &-\left[\tfrac{1}{16}J(\omega+3\omega_{DD})+\tfrac{1}{16}J(\omega-3\omega_{DD})\right]\rho_{22}\\ &-\left[\tfrac{1}{16}J(\omega+3\omega_{DD})+\tfrac{1}{16}J(\omega-3\omega_{DD})\right]\rho_{33}+\tfrac{1}{8}J(\omega-3\omega_{DD})\rho_{44}\\ &-\left[\tfrac{1}{8}J(\omega+3\omega_{DD})+\tfrac{1}{8}J(\omega-3\omega_{DD})+\tfrac{1}{12}J(0)\right]\rho_{23}+\tfrac{1}{12}J(0)\rho_{32}\end{aligned} \tag{14a}$$

$$\begin{aligned}\frac{d\rho_{32}}{dt} = &\,i\omega_{DD}\rho_{22}-i\omega_{DD}\rho_{33}+\tfrac{1}{8}J(\omega+3\omega_{DD})\rho_{11}\\ &-\left[\tfrac{1}{16}J(\omega+3\omega_{DD})+\tfrac{1}{16}J(\omega-3\omega_{DD})\right]\rho_{22}\\ &-\left[\tfrac{1}{16}J(\omega+3\omega_{DD})+\tfrac{1}{16}J(\omega-3\omega_{DD})\right]\rho_{33}\\ &+\tfrac{1}{8}J(\omega-3\omega_{DD})\rho_{44}+\tfrac{1}{12}J(0)\rho_{23}\\ &-\left[\tfrac{1}{8}J(\omega+3\omega_{DD})+\tfrac{1}{8}J(\omega-3\omega_{DD})+\tfrac{1}{12}J(0)\right]\rho_{32}\end{aligned} \tag{14b}$$

This gives a set of six coupled equations. Its numerical solution leads to a bi-exponential time evolution of the $\langle I_z\rangle = \langle I_{z,1}+I_{z,2}\rangle \propto (\rho_{44}-\rho_{11})$ quantity. Fig. 1 shows illustrative simulations of the two relaxation rates versus the resonance frequency assuming Lorentzian form of the spectral density function: $J(\omega) = (C_{DD})^2\frac{\tau_c}{1+(\omega\tau_c)^2}$, where C_{DD} denotes the amplitude of the fluctuating part of the dipole-dipole coupling. For $\omega_{DD} = 0$, Eqs. (13a-d,14a,b) converge to the well-known expressions for a system of two equivalent spin-1/2 nuclei [10-15].

4. Experimental examples and discussion

Experimental observation of the DRE effects is much more challenging than of QRE; there are three main reasons for that. The first one is the existence of a residual dipole-dipole interaction. The existence of a quadrupole interaction is guaranteed by the spin quantum number of the nucleus (being larger than 1/2), provided there is an electric field gradient at the nucleus site (that is almost always the case). A residual dipolar coupling is present only in specific cases, likely associated with anisotropic dynamics. The second reason is the low frequency at which the effect appear. Relaxation experiments at low frequencies are more difficult, with inherently low signal-to-noise ratios and, hence, the experimental error is larger. Eventually, the potential DRE peak can be masked by other relaxation contributions that lead to large relaxation rates at low frequencies. However, the relaxation features presented below can be explained by the DRE effect.

Fig. 2 shows ^{1}H spin-lattice relaxation data for L-asparagine – ^{15}N in powder collected in the frequency range from 4 kHz to

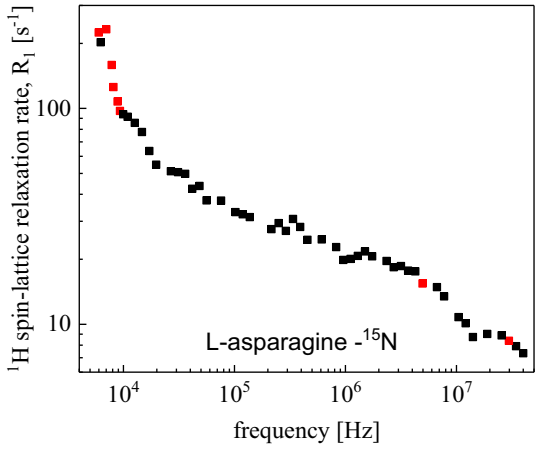

Fig. 2. ^{1}H spin-lattice relaxation data for L-asparagine-^{15}N in powder at 295 K. Red points – data selected for Fig. 3. (For interpretation of the references to colour in this figure legend, the reader is referred to the web version of this article.)

40 MHz. The use of ^{15}N instead of ^{14}N ensures that there are no QRE effects that potentially could affect the picture. The compound was purchased from Sigma Aldrich in the form of lyophilized powder. The ^{1}H spin-lattice relaxation rates were measured using a commercial relaxometer (Stelar srl., Italy, Spinmaster 2000). The magnetization values were measured for 16 logarithmically spaced time sets, the span of which was readjusted at every relaxation field to optimize the sampling of the decay/recovery curves. Free induction decays were recorded at 16.3 MHz after single $\pi/2$ pulse ($t_{\pi/2} = 9\mu s$). 32 scans were accumulated, a recycle delay of 0.75 s was applied between the successive scans. For magnetic fields below 11 MHz pre-polarization at 25 MHz was applied for 0.75 s. Temperature was stabilized with an air flux system with the accuracy of 0.5 K.

The relaxation rates have been obtained as a result of single-exponential fits of the ^{1}H magnetization versus time. A closer inspection of the magnetization curves indicates, however, that at low frequencies the magnetization evolution is bi-exponential, while at higher frequencies the magnetization curves tend to become single-exponential. This effect is shown in Fig. 3. The curves a)-f) correspond to low frequencies and the relaxation process is bi-exponential, while the magnetization data shown in g) and h) have been collected at higher frequencies and they can be well reproduced in terms of a single-exponential model. One can consider different explanations of the bi-exponentiality. The asparagine molecule includes chemically non-equivalent hydrogen atoms – this could give rise to a bi-exponential relaxation. However, if so, one would rather expect this effect to be more pronounced at high frequencies due to a larger chemical shifts between the different pools of ^{1}H nuclei. Another explanation might be related to the presence of ^{15}N nuclei. According to the Solomon – Bloembergen- Morgan model [10-15] relaxation processes in systems containing different kinds of NMR active species are bi-exponential as a result of cross-relaxation effects. However, if so, the bi-exponentiality should be seen in the whole frequency range. Thus, we are rather of the opinion that the bi-exponentiality at low frequencies is caused by the presence of a residual dipole-dipole interaction.

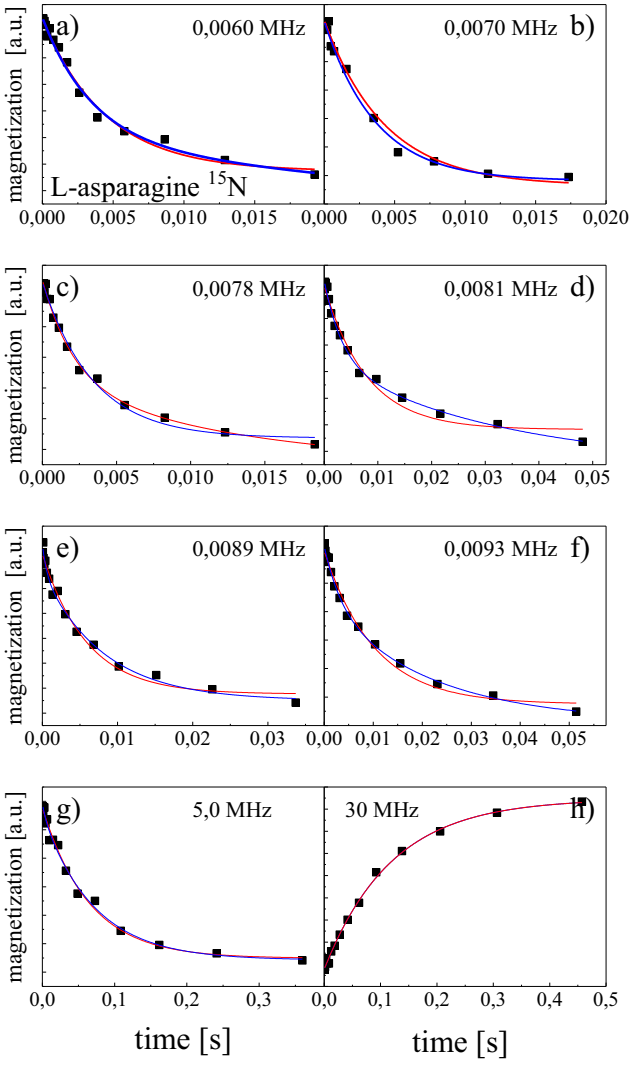

Fig. 3. ^{1}H magnetization versus time at selected frequencies. Red lines: single – exponential fits, blue lines: bi-exponential fits. (For interpretation of the references to colour in this figure legend, the reader is referred to the web version of this article.)

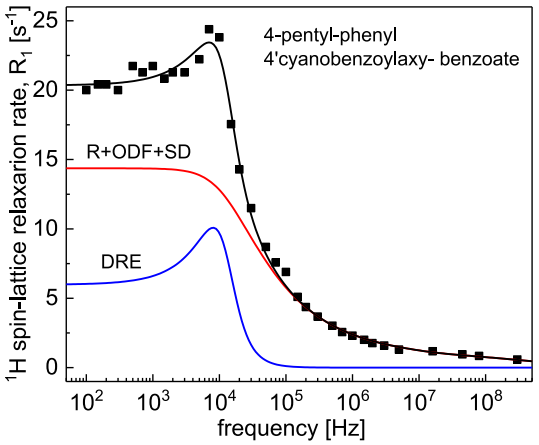

Fig. 4. ^{1}H spin-lattice relaxation data for 4-pentyl-phenyl 4′-cyanobenzoyloxy-benzoate at 423 K in the nematic phase [48].

Fig. 4 shows ^{1}H spin-lattice relaxation data for 4-pentyl-phenyl 4′-cyanobenzoyloxy-benzoate [47] in the nematic phase, already shown in Ref. [48,49].

The relaxation data have been successfully described by a sum of three main relaxation mechanisms: local rotations/reorientations, R, translational self-diffusion, SD, and collective motions described in terms of fluctuations of the alignment direction defined by an average over the molecular long axes of molecules (order director fluctuations), ODF [48,49]. The sum of these contributions is shown in Fig. 4. The well pronounced relaxation maximum at low frequencies has originally been attributed to QRE associated with ^{14}N nuclei present in the system [48]. However, in such a case one should be able to observe three quadrupole peaks at the frequencies of $\nu_- = \frac{\omega_-}{2\pi} = \frac{3}{4}a_Q(1-\frac{\eta}{3})$, $\nu_+ = \frac{\omega_+}{2\pi} = \frac{3}{4}a_Q(1+\frac{\eta}{3})$ and $\nu_0 = \nu_+ - \nu_- = \frac{\omega_0}{2\pi} = \frac{1}{2}\eta\, a_Q$ [27-34], where a_Q and η denote the amplitude and the asymmetry parameter of the quadrupole coupling, respectively. Such sets of quadrupole peaks have been observed for many systems [28-34], but always the higher frequency lines were more pronounced than the low frequency one. As in this case only a single relaxation maximum at low frequencies have been observed, one can suppose that it is rather caused by the DRE effect. The relaxation contribution attributed in [48] to the QRE is explicitly shown in Fig. 4. Its shape indeed closely resembles the simulated DRE presented in Fig. 2 indicating ω_{DD} being of the order of about $2^{*}10^{4}$ rad/s.

5. Conclusions

A model of spin-lattice relaxation for spin-1/2 nuclei in the presence of residual dipole-dipole interactions has been developed.

The model has led to two important conclusions. The first one is that for slow dynamics the spin-lattice relaxation becomes bi-exponential at low frequencies as a result of the residual dipole-dipole coupling. The second conclusion is that one of the relaxation components shows (for slow dynamics) a frequency-specific relaxation enhancement (dipolar relaxation peak) which we have described as Dipolar Relaxation Enhancement (DRE) in analogy to QRE. The bi-exponentiality of the relaxation process combined with the position of the dipolar relaxation peak (determined by the amplitude of the residual dipolar coupling) and its shape have the potential to provide unique information about molecular arrangement and dynamics, likely to be of importance for applications in materials science and medical diagnostics.

Declaration of Competing Interest

The authors declare that they have no known competing financial interests or personal relationships that could have appeared to influence the work reported in this paper.

Acknowledgement

This project has received funding from the European Union's Horizon 2020 research and innovation programme under grant agreement No 668119 (project "IDentIFY"). The role of COST Action CA15209 (European Network on NMR Relaxometry) is also acknowledged.

References

[1] R. Kimmich, E. Anoardo, Field-cycling NMR relaxometry, Prog. Nucl. Magn. Reson. Spectrosc. 44 (2004) 257–320, https://doi.org/10.1016/j.pnmrs.2004.03.002.
[2] F. Fujara, D. Kruk, A.F. Privalov, Solid state Field-Cycling NMR relaxometry: Instrumental improvements and new applications, Prog. Nucl. Magn. Reson. Spectrosc. 82 (2014) 39–69, https://doi.org/10.1016/j.pnmrs.2014.08.002.
[3] D. Kruk, A. Herrmann, E.A. Rössler, Field-cycling NMR relaxometry of viscous liquids and polymers, Prog. Nucl. Magn. Reson. Spectrosc. 63 (2012) 33–64, https://doi.org/10.1016/j.pnmrs.2011.08.001.
[4] J.-P. Korb, Multi-scales nuclear spin relaxation of liquids in porous media, Comptes Rendus Phys. 11 (2010) 192–203, https://doi.org/10.1016/j.crhy.2010.06.015.
[5] R. Meier, D. Kruk, E.A. Rössler, Intermolecular spin relaxation and translation diffusion in liquids and polymer melts: insight from field-cycling ^{1}H NMR relaxometry, ChemPhysChem 14 (2013) 3071–3081, https://doi.org/10.1002/cphc.201300257.
[6] D. Kruk, M. Florek-Wojciechowska, Recent development in 1H NMR relaxometry, Annu. Reports NMR Spectrosc. (2019) 1–66, https://doi.org/10.1016/bs.arnmr.2019.10.001.
[7] R. Meier, D. Kruk, J. Gmeiner, E.A. Rössler, Intermolecular relaxation in glycerol as revealed by field cycling 1H NMR relaxometry dilution experiments, J. Chem. Phys. 136 (2012), https://doi.org/10.1063/1.3672096 034508.
[8] D. Kruk, R. Meier, E.A. Rössler, Translational and rotational diffusion of glycerol by means of field cycling 1H NMR relaxometry, J. Phys. Chem. B. 115 (2011) 951–957, https://doi.org/10.1021/jp110514r.
[9] D. Kruk, P. Rochowski, E. Masiewicz, S. Wilczynski, M. Wojciechowski, L.M. Broche, D.J. Lurie, Mechanism of water dynamics in hyaluronic dermal fillers revealed by nuclear magnetic resonance relaxometry, ChemPhysChem 20 (2019) 2816–2822, https://doi.org/10.1002/cphc.201900761.
[10] A. Abragam, The Principles of Nuclear Magnetism, Oxford University Press, 1961.
[11] C.P. Slichter, Principles of Magnetic Resonance, third ed., Springer-Verlag, Berlin, 1990.
[12] J. Kowalewski, L. Maler, Nuclear Spin Relaxation in Liquids: Theory, Experiments, and Applications, second ed., Taylor & Francis, New York, 2006.
[13] N. Bloembergen, L.O. Morgan, Proton relaxation times in paramagnetic solutions. Effects of electron spin relaxation, J. Chem. Phys. 34 (1961) 842–850, https://doi.org/10.1063/1.1731684.
[14] A. Redfield, Relaxation theory: density matrix formulation, in: D. Grant, R. Harris (Eds.), Encycl. Nucl. Magn. Reson., Wiley, Chichester, 1996, pp. 4085–4092.
[15] D. Kruk, Understanding Spin Dynamics, Pan Stanford, 2015.
[16] L.-P. Hwang, J.H. Freed, Dynamic effects of pair correlation functions on spin relaxation by translational diffusion in liquids, J. Chem. Phys. 63 (1975) 4017, https://doi.org/10.1063/1.431841.
[17] Y. Ayant, E. Belorizky, J. Aluzon, J. Gallice, Calcul des densités spectrales résultant d'un mouvement aléatoire de translation en relaxation par interaction dipolaire magnétique dans les liquides, J. Phys. 36 (1975) 991–1004, https://doi.org/10.1051/jphys:019750036010099100.
[18] P.H. Fries, Dipolar nuclear spin relaxation in liquids and plane fluids undergoing chemical reactions, Mol. Phys. 48 (1983) 503–526, https://doi.org/10.1080/00268978300100361.
[19] E. Belorizky, P.H. Fries, A. Guillermo, O. Poncelet, Almost ideal 1D water diffusion in imogolite nanotubes evidenced by NMR relaxometry, ChemPhysChem 11 (2010) 2021–2026, https://doi.org/10.1002/cphc.200901030.
[20] J.-P. Korb, M. Winterhalter, H.M. McConnell, Theory of spin relaxation by translational diffusion in two-dimensional systems, J. Chem. Phys. 80 (1984) 1059–1068, https://doi.org/10.1063/1.446823.
[21] D. Kruk, R. Meier, E.A. Rössler, Nuclear magnetic resonance relaxometry as a method of measuring translational diffusion coefficients in liquids, Phys. Rev. E. 85 (2012), https://doi.org/10.1103/PhysRevE.85.020201 020201.
[22] C. Luchinat, G. Parigi, E. Ravera, Water and protein dynamics in sedimented systems: a relaxometric investigation, ChemPhysChem 14 (2013) 3156–3161, https://doi.org/10.1002/cphc.201300167.
[23] E. Ravera, G. Parigi, A. Mainz, T.L. Religa, C. Luchinat, Experimental determination of microsecond reorientation correlation times in protein solutions, J. Phys. Chem. B. 117 (2013) 3548–3553, https://doi.org/10.1021/jp312561f.
[24] G. Parigi, N. Rezaei-Ghaleh, A. Giachetti, S. Becker, C. Fernandez, M. Blackledge, C. Griesinger, M. Zweckstetter, C. Luchinat, Long-range correlated dynamics in intrinsically disordered proteins, J. Am. Chem. Soc. 136 (2014) 16201-16209. doi: 10.1021/ja506820r.
[25] E. Ravera, M. Fragai, G. Parigi, C. Luchinat, Differences in dynamics between crosslinked and non-crosslinked hyaluronates measured by using fast field-cycling relaxometry, ChemPhysChem 16 (2015) 2803–12089, https://doi.org/10.1002/cphc.201500446.
[26] G. Liu, M. Levien, N. Karschin, G. Parigi, C. Luchinat, M. Bennati, One-thousand-fold enhancement of high field liquid nuclear magnetic resonance signals at room temperature, Nat. Chem. 9 (2017) 676–680, https://doi.org/10.1038/nchem.2723.
[27] D. Kruk, A. Kubica, W. Masierak, A.F. Privalov, M. Wojciechowski, W. Medycki, Quadrupole relaxation enhancement–application to molecular crystals, Solid State Nucl. Magn. Reson. 40 (2011) 114–120, https://doi.org/10.1016/j.ssnmr.2011.08.003.
[28] M. Florek-Wojciechowska, M. Wojciechowski, R. Jakubas, S. Brym, D. Kruk, ^{1}H NMR relaxometry and quadrupole relaxation enhancement as a sensitive probe of dynamical properties of solids—$[C(NH_2)_3]_3Bi_2I_9$ as an example, J. Chem. Phys. 144 (2016), https://doi.org/10.1063/1.4940680 054501.
[29] M. Florek-Wojciechowska, R. Jakubas, D. Kruk, Structure and dynamics of [NH2(CH3)2]3Sb2Cl9 by means of 1H NMR relaxometry – quadrupolar relaxation enhancement effects, Phys. Chem. Chem. Phys. 19 (2017) 11197–11205, https://doi.org/10.1039/c7cp00788d.
[30] P.-O. Westlund, Quadrupole-enhanced proton spin relaxation for a slow reorienting spin pair: (I)–(S). A stochastic Liouville approach, Mol. Phys. 107 (2009) 2141–2148, https://doi.org/10.1080/00268970903185909.
[31] P.-O. Westlund, The quadrupole enhanced 1H spin–lattice relaxation of the amide proton in slow tumbling proteins, Phys. Chem. Chem. Phys. 12 (2010) 3136, https://doi.org/10.1039/b922817a.
[32] E.P. Sunde, B. Halle, Mechanism of 1H–14N cross-relaxation in immobilized proteins, J. Magn. Reson. 203 (2010) 257–273, https://doi.org/10.1016/j.jmr.2010.01.008.
[33] D. Kruk, E. Masiewicz, A.M. Borkowska, P. Rochowski, P.H. Fries, L.M. Broche, D. J. Lurie, Dynamics of solid proteins by means of nuclear magnetic resonance relaxometry, Biomolecules 9 (2019) 652, https://doi.org/10.3390/biom9110652.
[34] F. Winter, R. Kimmich, NMR field-cycling relaxation spectroscopy of bovine serum albumin, muscle tissue, micrococcus luteus and yeast. 14N1H-quadrupole dips, BBA - Gen. Subj. 719 (1982) 292–298. doi: 10.1016/0304-4165(82)90101-5.
[35] D.J. Lurie, S. Aime, S. Baroni, N.A. Booth, L.M. Broche, C.-H. Choi, G.R. Davies, S. R. Ismail, D.O. Hogain, K.J. Pine, Fast field-cycling, Magn. Reson. Imaging 11 (2010) 136, https://doi.org/10.1016/j.crhy.2010.06.012.
[36] D.J. Lurie, Quadrupole-Dips Measured by Whole-Body Field-Cycling Relaxometry and Imaging, in: Proc. Int. Soc. Magn. Reson. Med., 1999, p. 653.
[37] L.M. Broche, P.J. Ross, G.R. Davies, M.-J. MacLeod, D.J. Lurie, A whole-body Fast Field-Cycling scanner for clinical molecular imaging studies, Sci. Rep. 9 (2019) 10402, https://doi.org/10.1038/s41598-019-46648-0.
[38] D. Kruk, E. Umut, E. Masiewicz, C. Sampl, R. Fischer, S. Spirk, C. Goesweiner, H. Scharfetter, 209 Bi quadrupole relaxation enhancement in solids as a step towards new contrast mechanisms in magnetic resonance imaging, Phys. Chem. Chem. Phys. 20 (2018) 12710–12718, https://doi.org/10.1039/C8CP00993G.
[39] D. Kruk, E. Masiewicz, E. Umut, A. Petrovic, R. Kargl, H. Scharfetter, Estimation of the magnitude of quadrupole relaxation enhancement in the context of magnetic resonance imaging contrast, J. Chem. Phys. 150 (2019), https://doi.org/10.1063/1.5082177.
[40] D. Kruk, E. Umut, E. Masiewicz, R. Fischer, H. Scharfetter, Multi-quantum quadrupole relaxation enhancement effects in 209Bi compounds, J. Chem. Phys. 150 (2019), https://doi.org/10.1063/1.5082007.
[41] G. Lipari, A. Szabo, Model-free approach to the interpretation of nuclear magnetic resonance relaxation in macromolecules. 1. Theory and range of validity, J. Am. Chem. Soc. 104 (1982) 4546–4559, https://doi.org/10.1021/ja00381a009.

[42] R. Kimmich, NMR: Tomography, Diffusometry, Relaxometry, Springer Science & Business Media, Berlin, 1997.
[43] J. Jeener, Superoperators in magnetic resonance, in: Adv. Magn. Opt. Reson., Academic Press, 1982, pp. 1–51. doi: 10.1016/B978-0-12-025510-8.50006-1.
[44] D. Kruk, Theory of Evolution and Relaxation of Multi-spin Systems. Application to Nuclear Magnetic Resonance (NMR) and Electron Spin Resonance (ESR), Abramis Academic, Arima Publishing, UK, 2007.
[45] M. Goldman, Formal theory of spin-lattice relaxation, J. Magn. Reson. 149 (2001) 160–187, https://doi.org/10.1006/jmre.2000.2239.
[46] R.R. Ernst, G. Bodenhausen, A. Wokaun, Principles of Nuclear Magnetic Resonance in One and Two Dimensions, Clarendon Press, 1991.
[47] F. Hardouin, A.M. Levelut, J.J. Benattar, G. Sigaud, X-rays investigations of the smectic A1 - smectic A2 transition, Solid State Commun. 33 (1980) 337–340, https://doi.org/10.1016/0038-1098(80)91165-5.
[48] P.J. Sebastiao, A.C. Ribeiro, H.T. Nguyen, F. Noack, Proton NMR relaxation study of molecular motions in a liquid crystal with a strong polar terminal group, Zeitschrift Fur Naturforsch. - Sect. A J. Phys. Sci. 48 (1993) 851–860, https://doi.org/10.1515/zna-1993-8-903.
[49] P.J. Sebastião, Chapter 11: NMR Relaxometry in Liquid Crystals: Molecular Organization and Molecular Dynamics Interrelation, in: New Dev. NMR, Royal Society of Chemistry, 2018, pp. 255–302. doi: 10.1039/9781788012966-00255.